SIMULATION DOMAIN GENERATION FOR CHARACTERIZATION OF SHALE SOURCE ROCKS

Timothy I. Anderson, Bolivia Vega, Laura Frouté, Kelly Guan, & Anthony R. Kovscek
Department of Energy Resources Engineering
Stanford University
Stanford, CA 94305, USA
{timothy.anderson, bolivia, lfroute, kmguan, kovscek}@stanford.edu

ABSTRACT

Deep learning-based simulation techniques have shown stunning success across a wide range of applications in the energy and geosciences. A critical step in applying any simulation technique to the characterization of petroleum source rocks is obtaining a suitable simulation domain. In this work, we present image translation models that generate image volumes suitable for segmentation and visualization of gas flow through a shale rock volume. We introduce a regularization method for improving 3D volume generation when only 2D training data is available and present results applying this approach to calculating rock permeability from the synthesized simulation domains. Overall, our results show that deep learning-based image translation can play a crucial role in creating simulation domains for characterization of geologic samples.

1 INTRODUCTION

Shale gas resources are critical for the U.S. energy supply. Since 2009, shale gas has accounted for a majority of the increase in domestic energy production and contributed substantially to reduction in CO_2 emissions due to fuel switching (Zoback & Kohli, 2019; EIA/ARI, 2013). Rock features on length scales from $\mathcal{O}(10^{-9}$ m) to $\mathcal{O}(10^{+2}$ m) affect recovery in shales, and consequently nanoscale characterization techniques—especially nanoscale imaging—are important for understanding shale source rocks.

Nanoscale imaging in conjunction with digital rock physics allows for analysis and characterization of morphological and petrophysical properties of source rock samples (Ketcham & Carlson, 2001; Vega et al., 2013; Blunt, 2017). This characterization approach, however, faces two significant challenges. First, nanoscale image acquisition is typically expensive, time-consuming, and/or sample-destructive. Second, 3D image volumes are required to simulate petrophysical properties, but many imaging modalities that possess sufficiently high contrast and resolution to build useful nanoscale simulation domains, such as electron microscopy, only acquire 2D planar images. Consequently, we must reconstruct realistic 3D simulation domains when only 2D ground truth training data is available.

In this work, we apply image translation models to generate 3D simulation domains for calculating rock permeability from non-destructive 2D image data. In what follows, we present a multimodal image acquisition and prediction workflow based on conditional generative adversarial networks (CGANs), a modification of baseline CGAN models to improve volume generation, and simulation of flow through a segmented image volume.

2 METHODOLOGY

2.1 IMAGE-BASED CHARACTERIZATION WORKFLOW

Image-based characterization for source rocks is most broadly defined as the process of acquiring, processing, and analyzing the images using digital rock physics techniques. This workflow approximately follows these steps:

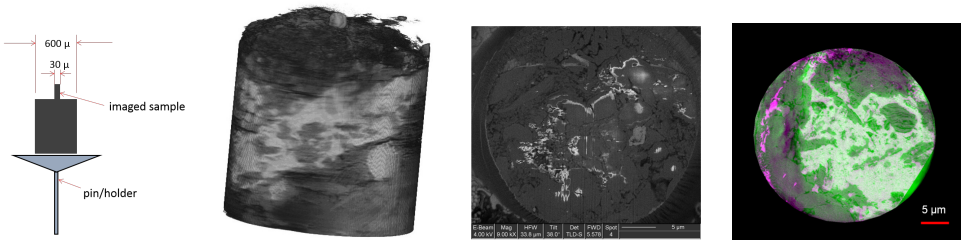

(a) (b) (c) (d)

Figure 1: Multimodal imaging dataset. (a) Sample setup, (b) Imaged nano-CT volume of 30 µm diameter plug, (c) Unprocessed FIB-SEM image slice, (d) Example of paired nano-CT/SEM-FIB image slice overlay.

Image Acquisition → Data Curation and Model Training →
Image Prediction and Domain Generation → Analysis and Simulation

Multimodal imaging, where images of a sample are acquired at the same resolution scale with two different image modalities, is an emerging and important area for shale characterization (Aljamaan et al., 2017). In a multimodal image characterization workflow, images are acquired on multiple imaging machines and deep learning models trained to predict one modality from the other. The predicted images are then post-processed into a simulation domain that can be used to compute morphological properties such as Minkowski functionals or petrophysical properties including apparent permeability (Arns et al., 2010).

While multimodal imaging is commonplace in medical imaging (Torrado-Carvajal et al., 2016; Cao et al., 2018), little prior work has applied multimodal imaging to the characterization of source rocks. Nanoscale imaging modalities useful for shale characterization present a trade-off between resolution and sample destruction. High-resolution/high-contrast methods often destroy samples to acquire image volumes, while sample-preserving methods have comparatively lower contrast and resolution. Multimodal imaging offers the potential to predict high-resolution images suitable for segmentation and simulation from low-resolution, non-destructive images.

2.2 Multimodal Imaging Dataset

In this work, we use a dual modality nano-computed tomography (nano-CT) and focused ion beam scanning electron microscopy (FIB-SEM) dataset of a shale sample from the Vaca Muerta formation, one of the most prolific shale plays. After preliminary imaging, the sample is milled to a 30 µm diameter plug (Fig. 1a) and imaged with nano-CT (Fig. 1b). The plug is then sequentially milled into and imaged with scanning electron microscopy (Fig. 1c). The image slices from both modalities are then aligned, normalized, and cropped to produce a paired multimodal image dataset (Fig. 1d). Further details on this dataset are outlined in Anderson et al. (2020).

Darker pixel values in these images indicate low density material, with the darkest pixels corresponding to fractures, organic matter and low density minerals. Flow in shales occurs through pore networks located in organic matter and low density mineral regions, so these regions make up the flow simulation domain. Lower density regions, however, are not well resolved on the nano-CT images, so we must employ image translation models to predict FIB-SEM images from nano-CT data and to synthesize low density regions from nondestructive images. The synthesized lower density regions can then be segmented into a suitable simulation domain to measure rock properties.

2.3 Image Volume Synthesis and Domain Generation

To generate low density regions for a simulation domain, we turn to image translation models. The image acquisition environment restricts the data to 2D paired images, so we are limited to 2D-to-2D image prediction models. Predicting FIB-SEM images from nano-CT data is a combination of

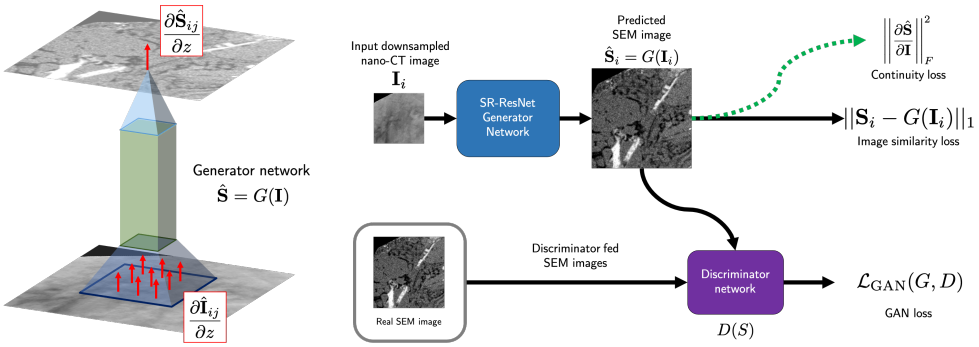

Figure 2: Image prediction model. (a) Depiction of nano-CT image gradients propagating through the generator network to the output image, (b) SR-GAN model with Jacobian regularization term.

image domain translation and single image super-resolution (SISR). Therefore, we apply the SR-GAN model from Ledig et al. (2016) because it is a useful baseline model for SISR.

To improve image volume generation, we first note that $\nabla_z \boldsymbol{S}$ will be sparse for any SEM image $\boldsymbol{S}$. Therefore, we enforce continuity in the predicted image volumes by regularizing with $||\nabla_z \boldsymbol{S}||_1$. This term, however, is not easily computed. For $\hat{\boldsymbol{S}} = G(\boldsymbol{I})$, where $\hat{\boldsymbol{S}}$ is the predicted SEM image and $\boldsymbol{I}$ is the input nano-CT image, we observe that

$$||\nabla_z \hat{\boldsymbol{S}}||_1 \leq C \left|\left| \frac{\partial \hat{\boldsymbol{S}}}{\partial \boldsymbol{I}} \right|\right|_F^2 \equiv \mathcal{L}_{\text{Continuity}}(G)$$

and therefore we can improve the z-direction continuity through Jacobian regularization. A depiction of this regularization approach is shown in Fig. 2a. Using this Jacobian regularization term, the training objective for the GAN models becomes:

$$G^*, D^* = \underset{G,D}{\text{minimize}}\ \mathcal{L}_{\text{GAN}}(G, D) + \lambda_1 \mathcal{L}_{\text{Image Similarity}}(G) + \lambda_2 \mathcal{L}_{\text{Continuity}}(G)$$

The SR-GAN model with the continuity loss is shown in Fig. 2b. This approach is inspired by work on robust learning (Hoffman et al., 2019) and is comparable to regularizing the model to reduce the sensitivity of network outputs to inputs.

Finally, we use threshold-based segmentation to create the final flow simulation domain. The histogram of pixel values in FIB-SEM images corresponds directly to different mineral types and is proportional to the density of materials. So, thresholding is appropriate for creating a simulation domain consisting of lower-density regions. We threshold the volume using the smallest voxel value that creates a connected domain from the inlet to the outlet of the volume in the z-direction.

3 Results

Synthesized image volumes using the baseline and regularized SR-GAN models are shown in Fig. 3. These volumes are synthesized by first training 2D-to-2D image generation models, then passing $x-y$ plane image slices of the nano-CT volume through the generator network. The $x-y$ images are therefore generated independently. In the synthesized volumes, we see that the regularized model produces more continuous image features across slices.

The segmentation into a flow simulation domain of the volume synthesized with the regularized SR-GAN model is shown in Fig. 4a. We simulate flow in the z-direction by using a permeability solver in the PerGeos software. The simulation solves the Stokes equation using Finite Volume (FV) discretization. Methane is introduced from the inlet at 1 MPa, with a 10^{-2} MPa pressure drop in the z-direction. An additional volume is included at the inlet for pressure stabilization. No-flow

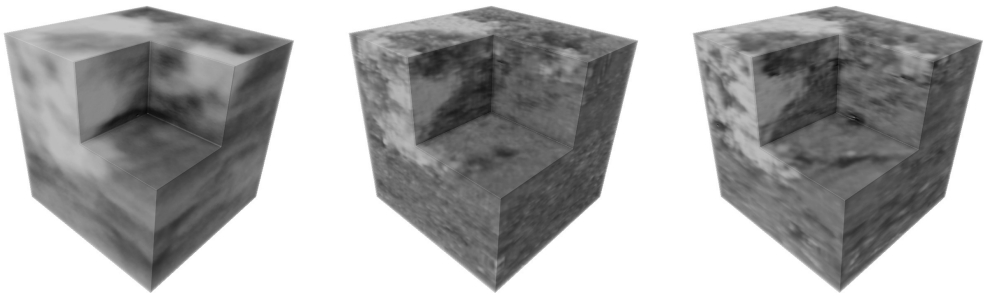

(a) (b) (c)

Figure 3: Image volume synthesis results for SR-GAN model. (a) Input nano-CT volume, (b) Synthesized image volume without regularization, and (c) Synthesized image with regularization. Lighter shading indicates more dense minerals.

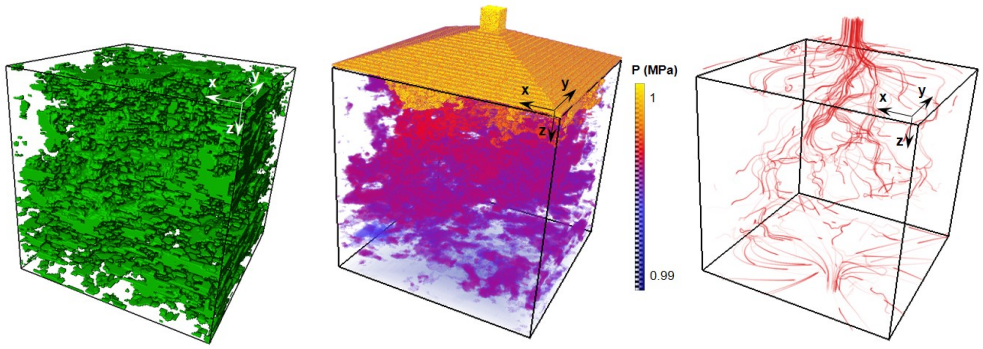

(a) (b) (c)

Figure 4: Flow simulation results for the regularized model. (a) Simulation domain (low density regions), (b) Pressure field (including the additional inlet volume), (c) Flow streamlines.

Table 1: Comparison of the flow properties predicted by the original and regularized SR-GAN models. The permeability k, total porosity ϕ, and connected porosity $\phi_{\text{connected}}$ are from PerGeos.

Model	k (d)	ϕ	$\phi_{\text{connected}}$
Original	2.37×10^{-5}	20.7%	18.7%
Regularized	3.01×10^{-5}	18.9%	17.4%

lateral boundaries and single-phase viscosity (not adjusted for the role of confinement) are imposed. The resulting pressure field and flow streamlines are shown in Fig. 4b and Fig. 4c. The results for apparent permeability (measured by Darcy's law) and porosity appear in Table 1.

4 Discussion and Conclusions

The image volume generation results show that the Jacobian regularization significantly improves the quality of the predicted image volume. We assume that at this scale, rock image features should be approximately isotropic, so $x - y$ plane slices should resemble $x - z$ and $y - z$ plane slices. The cross-sections in the regularized volumes qualitatively resemble the image generation planes, showing that the regularization method proposed here improves volume generation with 2D-to-2D image models. Indeed, we see that the apparent permeability for the regularized image volume is also higher than that for the baseline volume, further suggesting that that the regularization technique improves continuity in the z-direction.

Overall, our results show that it is possible to synthesize suitable simulation domains for visualizing gas flow through rock volumes using only 2D data during training and non-destructive image data during evaluation. Future work on this project should focus on additional processing to improve the appearance of the cross-sectional image planes. Because we can obtain simulation domains directly from non-destructive data, this image generation approach can be used to train models to predict pressure fields and streamlines directly from nano-CT data. Finally, we believe there are opportunities to employ the flow simulation as a prior to improve simulation domain synthesis.

Author Contributions

TA developed the image prediction model, BV acquired and curated the dataset, LF performed the simulations, KG assisted with model implementation and evaluation, and AK was the principal investigator on this work.

Acknowledgments

Thank you to Dr. C. M. Ross, M. Murugesu, and Y. Perez-Claro for helpful discussions related to this work. This work was supported as part of the Center for Mechanistic Control of Water-Hydrocarbon-Rock Interactions in Unconventional and Tight Oil Formations (CMC-UF), an Energy Frontier Research Center funded by the U.S. Department of Energy (DOE), Office of Science, Basic Energy Sciences (BES), under Award # DE-SC0019165. Code for this project is available at `https://github.com/supri-a/TXM2SEM`. Our implementation is based on the framework provided by Isola et al. (2017) and Zhu et al. (2017).

References

Hamza Aljamaan, Cynthia M Ross, and Anthony R Kovscek. Multiscale imaging of gas storage in shales. *SPE Journal*, 22(06):1–760, 2017.

Timothy I Anderson, Bolivia Vega, and Anthony R Kovscek. Multimodal imaging and machine learning to enhance microscope images of shale. *Computers and Geosciences*, 145(June):104593, 2020. ISSN 0098-3004. doi: 10.1016/j.cageo.2020.104593. URL `https://doi.org/10.1016/j.cageo.2020.104593`.

C. H. Arns, M. A. Knackstedt, and K. Mecke. 3D structural analysis: Sensitivity of Minkowski functionals. *Journal of Microscopy*, 240(3):181–196, 2010. ISSN 00222720. doi: 10.1111/j.1365-2818.2010.03395.x.

Martin J. Blunt. *Multiphase Flow in Permeable Media: A Pore-Scale Perspective*. Cambridge University Press, 2017. doi: 10.1017/9781316145098.

Xiaohuan Cao, Jianhuan Yang, Li Wang, Zhong Xue, Qian Wang, and Dinggang Shen. Deep learning based inter-modality image registration supervised by intra-modality similarity. In *International Workshop on Machine Learning in Medical Imaging*, pp. 55–63. Springer, 2018.

EIA/ARI. Eia/ari world shale gas and shale oil resource assessment. 2013. URL `https://www.eia.gov/analysis/studies/worldshalegas/archive/2013/pdf/fullreport_2013.pdf`.

Judy Hoffman, Daniel A. Roberts, and Sho Yaida. Robust learning with jacobian regularization, 2019.

Phillip Isola, Jun Yan Zhu, Tinghui Zhou, and Alexei A. Efros. Image-to-image translation with conditional adversarial networks. *Proceedings - 30th IEEE Conference on Computer Vision and Pattern Recognition, CVPR 2017*, 2017-Janua:5967–5976, 2017. doi: 10.1109/CVPR.2017.632.

Richard A. Ketcham and William D. Carlson. Acquisition, optimization and interpretation of x-ray computed tomographic imagery: Applications to the geosciences. *Computers and Geosciences*, 27(4):381–400, 2001. ISSN 00983004. doi: 10.1016/S0098-3004(00)00116-3.

Christian Ledig, Lucas Theis, Ferenc Huszar, Jose Caballero, Andrew Cunningham, Alejandro Acosta, Andrew Aitken, Alykhan Tejani, Johannes Totz, Zehan Wang, and Wenzhe Shi. Photo-Realistic Single Image Super-Resolution Using a Generative Adversarial Network. 2016. ISSN 0018-5043. doi: 10.1109/CVPR.2017.19.

A. Torrado-Carvajal, J. L. Herraiz, E. Alcain, A. S. Montemayor, L. Garcia-Canamaque, J. A. Hernandez-Tamames, Y. Rozenholc, and N. Malpica. Fast Patch-Based Pseudo-CT Synthesis from T1-Weighted MR Images for PET/MR Attenuation Correction in Brain Studies. *Journal of Nuclear Medicine*, 57(1):136–143, 2016. ISSN 0161-5505. doi: 10.2967/jnumed.115.156299.

Bolivia Vega, Joy C Andrews, Yijin Liu, Jeff Gelb, and Anthony Kovscek. Nanoscale visualization of gas shale pore and textural features. In *Unconventional resources technology conference*, pp. 1603–1613. Society of Exploration Geophysicists, American Association of Petroleum, 2013.

Jun Yan Zhu, Taesung Park, Phillip Isola, and Alexei A. Efros. Unpaired Image-to-Image Translation Using Cycle-Consistent Adversarial Networks. *Proceedings of the IEEE International Conference on Computer Vision*, 2017-Octob:2242–2251, 2017. ISSN 15505499. doi: 10.1109/ICCV.2017.244.

Mark D Zoback and Arjun H Kohli. *Unconventional reservoir geomechanics*. Cambridge University Press, 2019.